Mass and β Decay of ^{25}Ne, a $T_z = +\frac{5}{2}$ Nuclide*

David R. Goosman and D. E. Alburger
Brookhaven National Laboratory, Upton, New York 11973

and

J. C. Hardy
Brookhaven National Laboratory, Upton, New York 11973,
and Atomic Energy of Canada Limited, Chalk River Nuclear Laboratories, Chalk River, Ontario, Canada

(Received 7 December 1972)

The first reported measurement of the delayed γ-ray spectrum following the β decay of ^{25}Ne is presented. ^{25}Ne recoils from the ^{9}Be(^{18}O, $2p$)^{25}Ne reaction were thermalized in He gas and transferred through traps to a remotely located counting station. γ and β rays were counted simultaneously with Ge(Li) and NE102 detectors, respectively. γ-ray energies (in keV) and relative intensities for the ^{25}Na daughter transitions are 89.53 ± 0.10 (95.5 ± 0.6), 979.77 ± 0.16 (18.1 ± 1.9), 1069.30 ± 0.19 (2.34 ± 0.38), 2112.5 ± 1.0 (0.62 ± 0.19), 2202.0 ± 1.0 (1.1 ± 0.3), and 3688 ± 3 (0.96 ± 0.24). The ground-state β branch has been measured to be less than 20% of all β branches. The ^{25}Na excitation energies (in keV) and β branches (in %, assuming the ground-state branch is zero) are 89.53 ± 0.10 (76.8 ± 1.9), 1069.32 ± 0.19 (19.2 ± 2.0), 2202 ± 1 (2.3 ± 0.5), and 3688 ± 3 (1.18 ± 0.30). A 0.52 ± 0.15% branch is tentatively assigned to a state in ^{25}Na at 4289 ± 3 keV, on the basis of an observed 3220 ± 3-keV γ ray. The half-life of ^{25}Ne has been measured to be 602 ± 8 msec. By measuring the end-point energy of the β spectrum populating the first excited state of ^{25}Na the mass excess of ^{25}Ne has been measured to be −1.96 ± 0.30 MeV. Comparison of the mass and decay of ^{25}Ne with theoretical estimates and models is made.

I. INTRODUCTION

It has recently[1] been noted and demonstrated that heavy-ion compound reactions are a useful tool for producing very neutron-rich ($T_z = +\frac{5}{2}$ and +3) nuclides in the s-d shell. The study of such nuclei is important because mass measurements far from the valley of stability provide a sensitive test of various empirical mass formulas which fit the measured masses near the bottom of the valley of stability but which may diverge farther away. Also, decay measurements provide insight into the nuclear structure of both parent and daughter nuclides through the Gamow-Teller matrix elements, and check that conventional nuclear models can qualitatively explain the structure of light nuclei with high T_z.

This article presents the first reported measurement of the mass of ^{25}Ne and its delayed γ rays. This is the third $T_z = +\frac{5}{2}$ nuclide in the s-d shell to be studied via heavy-ion compound reactions. The first two members of this class to be populated in this way were ^{33}Si (Ref. 2) and ^{35}P (Ref. 3). The remaining members of the $T_z = +\frac{5}{2}$ series, ^{21}O, ^{23}F, ^{27}Na, ^{29}Mg, and ^{31}Al have not yet been produced by compound reactions, but studies of these nuclei are being undertaken. To date, no members of the $T_z = +3$ series, ^{22}O, ^{24}F, ^{26}Ne, ^{28}Na, ^{30}Mg, ^{32}Al, and ^{34}Si have been studied via compound reactions, although ^{22}O, ^{26}Ne, ^{30}Mg, and ^{34}Si are accessible by reasonable heavy-ion compound reactions, i.e., ^{10}Be(^{18}O, $\alpha 2p$), ^{10}Be(^{18}O, $2p$), ^{14}C(^{18}O, $2p$), and ^{18}O(^{18}O, $2p$), respectively. These nuclides were shown to be nucleon stable via heavy-ion transfer reactions by Artukh *et al.*,[4,5] and via high-energy proton spallation reactions by Klapisch *et al.*[6] The half-lives and singles β-ray spectra of ^{27}Na and ^{28}Na have been reported also by Klapisch *et al.*[6]

^{25}Ne was first shown to be nucleon stable by Artukh *et al.*,[4] and recently Kabachenko *et al.*[7] have bombarded tantalum and thorium foils with 180-MeV ^{22}Ne ions, observing the time and pulse-height distribution of events in a stilbene scintillator located at the mass-25 position of their on-line isotope separator. After removing a long-lived component with $T_{1/2} = 61.0 \pm 0.9$ sec (from ^{25}Na) from their time distribution, they report a short-lived activity with $T_{1/2} = 642 \pm 14$ msec, which they attributed to ^{25}Ne formed by three-neutron transfer to the incident ^{22}Ne ion. They also reported a β end point of 7.1 ± 0.3 MeV for the short-lived activity, which is consistent with the Garvey *et al.*[8] estimate for ^{25}Ne. This represents all of the information known to the authors concerning ^{25}Ne at the time of the present work. Figure 1 shows the previously reported information concerning ^{25}Ne and ^{25}Na. The half-life for ^{25}Ne is from Ref.

7, and the Q_β estimate of 7.4 MeV is that of Garvey *et al.*[8] The spherical shell model predicts a spin of $\frac{1}{2}^+$ for the ground state of ^{25}Ne. This prediction is strengthened by the fact that there is no known β^- emitter with odd mass from mass 19 through 35 (the s-d shell) whose spin is known to disagree with the spherical shell-model prediction. Even for very neutron-rich nuclei such as ^{33}Si and ^{35}P, where the spin is not certain, the β decay is consistent with the shell-model spin prediction.[2,3]

The information concerning ^{25}Na is taken from the summary by Becker *et al.*,[9] except that a level at 4286 keV reported by Hinds, Marchant, and Middleton[10] has been included. The 90-keV level most likely has a spin of $\frac{3}{2}^+$, although $\frac{5}{2}^+$ is possible, because of the decided preference for the 1068-keV level to cascade through it. From Fig. 1 one sees that if the spin of ^{25}Ne is $\frac{1}{2}^+$, then β decay to the ^{25}Na ground state is second forbidden. Then the β-ray end point of 7.1 ± 0.3 MeV for ^{25}Ne reported by Kabachenko *et al.*[7] would be a mixture of β transitions all leading to excited levels of ^{25}Na. One of the purposes of this work was to study the delayed γ-ray spectrum and to measure the spectra of coincident β rays to determine a mass excess for ^{25}Ne.

II. APPARATUS

Preliminary runs searching for delayed γ rays from ^{25}Ne were carried out with a thick Be target mounted in the Brookhaven National Laboratory (BNL) rabbit system which has been described previously.[1] The activity from the 1-min ^{25}Na isotope formed by ^{9}Be(^{18}O, pn)^{25}Na limited the usable beam current to about 60 nA of the 5^+ charge state. No evidence for ^{25}Ne was seen at 40-MeV ^{18}O energy.

In order to reduce the counting rate from ^{25}Na and also from ^{19}O produced by one-neutron transfer on ^{9}Be, the rabbit system was replaced by a gas-transfer system[11] shown in Fig. 2. The ^{18}O beam traversed a 2.10 ± 0.05-mg/cm^2-thick Be foil, which served both as the target and as a retaining window for 1 atm of He gas. At 44-MeV incident ^{18}O energy, ^{25}Ne recoils from the ^{9}Be(^{18}O, $2p$) reaction have just enough energy when produced near the vacuum side of the foil to traverse the entire foil and stop in the He gas. ^{25}Ne recoils produced near the gas side of the foil emerge with an energy of about 19 MeV but are still stopped by the He. According to the tables of Northcliffe and Schilling[12] the target thickness corresponds to an energy loss of 17 MeV in the lab or 5.7 MeV in the c.m. system for the incident ^{18}O beam. The Be foil was found to be very sturdy and withstood beams of 1 μA (electrical) of 44-MeV ^{18}O ions in the 5^+ charge state with no visible deterioration provid-

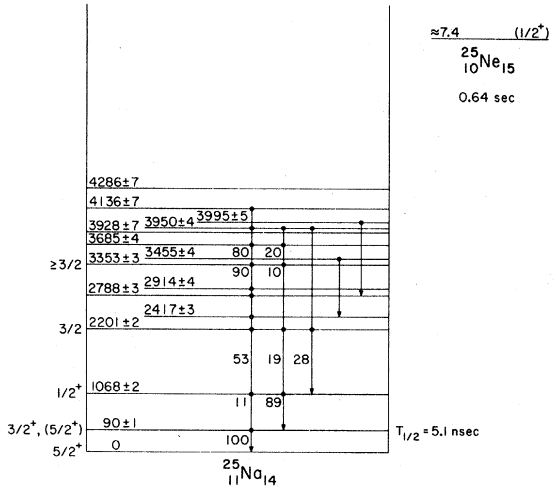

FIG. 1. Previously reported information concerning ^{25}Ne and ^{25}Na. Excitation energies (in keV) are from Refs. 9 and 10. The branches for the γ-ray decay of the 1069-keV level are a revision of the values quoted in Ref. 9.

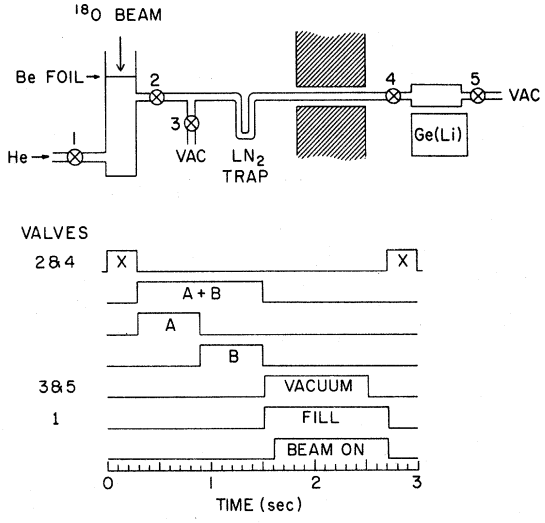

FIG. 2. The gas-transfer system. Helium is admitted to the target cell through valve 1 and then passes through a liquid nitrogen trap, through a 1.3-m-thick concrete shielding wall and into a counting cell located in the adjacent room. The distance between target and counting cells is 6 m. The counting cell, which is shown in simplified form, actually used three different geometries at the counting position. A typical timing sequence diagram illustrates valves 2 and 4 opening to start the sequence, two counting periods denoted A and B, an evacuation period when valves 3 and 5 are open, as well as filling and bombardment periods.

ed the bombardment was restricted to times when the target cell was filled with He.

The target cell was 10 cm long and 1.6 cm in diameter and was connected to the transfer tubing via electrically operated valves, numbered 1–5 in Fig. 2. The transfer tubing, trap, and counting cell were evacuated just prior to the end of the irradiation. By opening valves 2 and 4, with 1, 3, and 5 closed, the gas in the target cell expands through the trap into the counting cell. Timing for a typical cycle is shown in the lower part of Fig. 2.

This gas-transfer system is ideal for Ne recoils and has many advantages over the conventional rabbit system for gaseous activities. The greatest advantage is that long-lived activities can be pumped out each cycle (to the extent that they do not stick to the walls of the counting cell). In principle this should reduce the relative strength of the ^{25}Na activity by a factor of about 100 (as compared with the rabbit), which is the ratio of the half-lives of ^{25}Na and ^{25}Ne. Similarly, ^{19}O activity is reduced by a factor of 40. The cold trap further reduces ^{25}Na and ^{24}Na activities.

Timing for the cyclic sequence of events was provided by a 10-channel crystal-controlled programmer,[13] which controlled both the transfer system and an on-line computer for data storage.

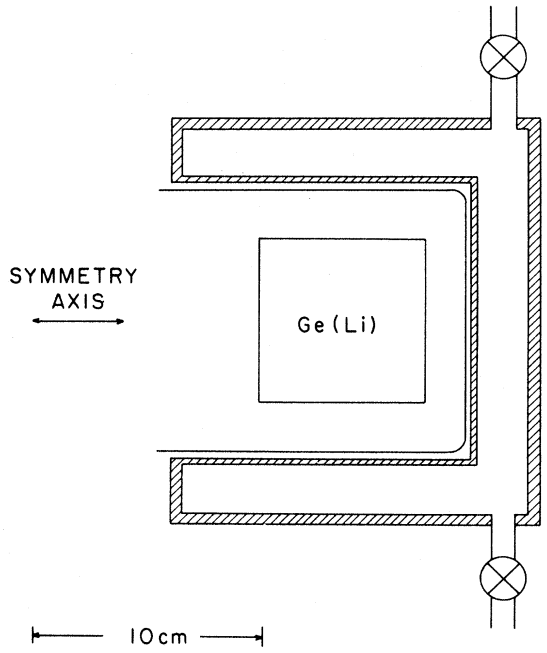

FIG. 3. The counting cell used in geometry 1. This is a cross-sectional view of the cell, which is azimuthally symmetric about the denoted symmetry axis, except for the valves. The square labeled "Ge(Li)" shows the location of the boundaries of the germanium ingot of the γ-ray detector. The U-shaped line surrounding this square is the aluminum container for the detector.

III. RESULTS WITH GEOMETRY 1

The fraction of the ^{25}Ne produced in the target cell that expands into the counting cell increases with the volume of the counting cell. The first runs taken with the gas-transfer system were done with the counting cell shown in Fig. 3, which has an internal volume of 450 cm^3 for good efficiency of transfer, while maintaining a close proximity to the 65-cm^3 Ge(Li) γ-ray detector. The internal walls of the counting cell were made of 1.5-mm-thick aluminum, in order to cause minimum attenuation for the anticipated 90-keV γ rays from the decay of ^{25}Ne (see Fig. 1). For geometry 1 runs, the transfer tubing was made of copper tubing 7.6-mm i.d. and the volumetric efficiency of the counting cell for this system was about 70%. Not shown in Fig. 3 are a brass x-ray shield surrounding the counting cell and 5 cm of lead shielding to reduce room background. The timing sequence diagram shown in Fig. 2 was modified in order to accomodate six sequential 0.65-sec counting periods following by an evacuation period of 0.9 sec.

These runs showed the presence of a strong 89.5-keV γ ray with a half-life near 0.6 sec. In Figs. 4 and 5 the spectra of the two strongest γ rays from the decay of ^{25}Ne are presented. The data of these figures were taken with a different geometry, but illustrate the quality of the results.

Of particular note is the comparison in Fig. 5 of the relative yields of ^{25}Na and ^{25}Ne taken with the gas-transfer system and with the conventional rabbit system.[1] We estimate that the ^{25}Na activity with the gas system is lower than with the rabbit system by a factor of about 400.

The delayed γ-ray spectrum contained lines from ^{19}O from one-neutron transfer, some ^{25}Na and ^{24}Na from the (^{18}O, pn) and (^{18}O, $p2n$) reactions, respectively, and lines from the decay of ^{23}Ne, ^{24}Ne, and ^{25}Ne. No other activities were observed.

The half-life extracted for the 89.5-keV line is shown in Fig. 6. The yield in each of the six time bins was corrected for dead time and other possible systematic effects by examining the yield of the prominent 197-keV line from ^{19}O. After corrections were made for the ^{19}O half-life, the dead-time corrections were calculated and amounted to about 1% for the first time bin. The dead time was low because the total γ-ray counting rate was only 500 counts/sec for a 1-μA beam current. This is to be compared with a total rate of about 10^4/sec at 60 nA for the rabbit system, with a similar target. The half-life deduced for ^{25}Ne is 602 ± 8 msec where the uncertainty is twice the statistical uncertainty in the fitted half-life, and encompasses slightly different computed half-lives obtained by

using different background fitting procedures. This result is in contrast to the value of 642 ± 14 msec reported by Kabachenko *et al.*[7] These authors obtained their value by observing the time distribution of pulses in a stilbene scintillator located at the mass-25 position of their on-line separator, after removing a long-lived component due to ^{25}Na.

Figure 7 shows the high-energy γ rays from the decay of ^{25}Ne taken in geometry 1 along with measured half-lives for these lines. These data were taken with a lower gain than that shown in Figs. 4 and 5, and represent the sum of data taken in three consecutive 0.6-sec time bins. These lines all correspond to known transitions in the level scheme of ^{25}Na shown in Fig. 1 with the exception of the 3220-keV line which is tentatively assigned as being due to a transition from the ^{25}Na 4286 ± 7-keV level to the 1069-keV level. This suggested assignment is based on the energy of the γ ray, the rough half-life which is consistent with that of ^{25}Ne, and because it is the only line in the spectrum which otherwise cannot be identified. No other transitions up to 6 MeV are seen in the low-gain runs.

Relative intensities for the ^{25}Na transitions were obtained by using the published[14,15] relative intensities of the ^{24}Na, ^{25}Na, and ^{19}O lines which were also present in the spectrum. A relative efficiency curve ranging from 110 to 2750 keV was obtained this way. These geometry 1 results suggested a relative γ-ray intensity of about 17% for the 979-keV line compared to the 89.5-keV line, indicating a rather sizable β-ray branch to the 1069-keV level in ^{25}Na. However, in geometry 1 the summing

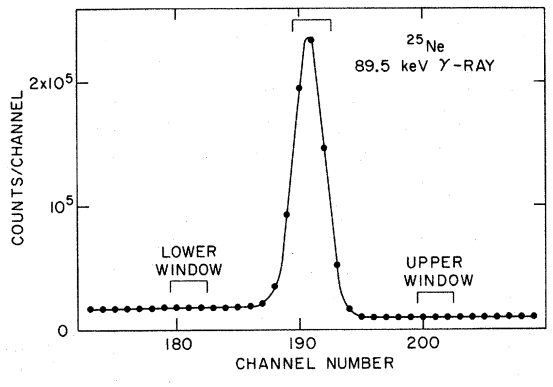

FIG. 4. Part of the delayed γ-ray spectrum from the bombardment of ^{9}Be with 44-MeV ^{18}O ions, showing the strongest line from the decay of ^{25}Ne, taken with geometry 3. The peak is 1.3 keV FWHM, and represents the counts occurring during the two successive 0.6-sec intervals. The brackets indicating lower, peak, and upper windows show where digital windows were set for later β-γ coincidence work.

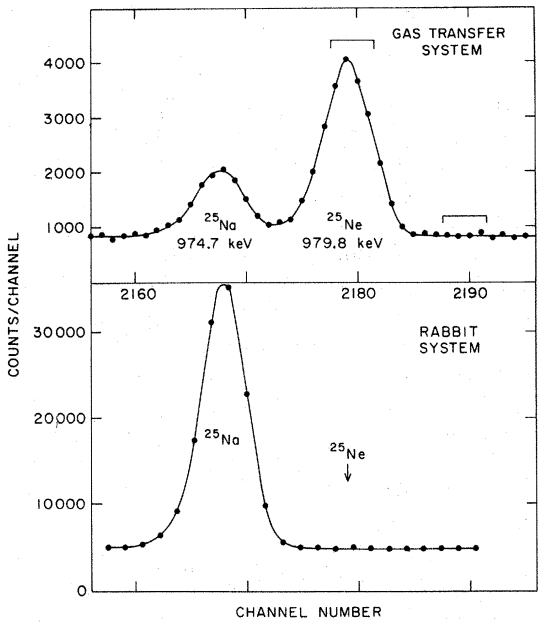

FIG. 5. Comparison of the yield of the 979.8-keV and 974.7-keV lines from ^{25}Ne and ^{25}Na, taken with the gas transfer and rabbit systems. The arrow on the lower curve shows where the ^{25}Ne(979) peak should be. The horizontal brackets on the upper curve show the location of digital windows used for β-γ coincidence work. The upper curve was taken in geometry 3.

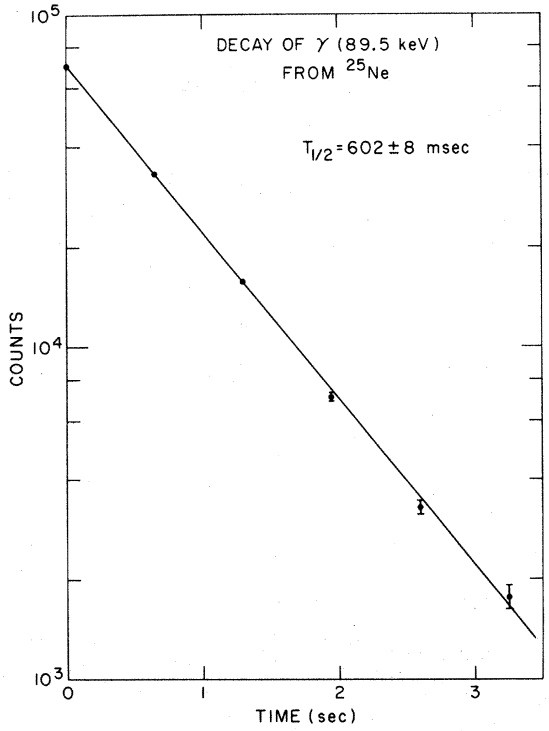

FIG. 6. Decay curve for the 89.5-keV γ ray, taken with geometry 1.

effects are such that if a 979-keV γ ray loses all its energy in the Ge(Li) detector, there is about a 6% chance that the associated 89-keV γ ray will leave some energy in the detector, thus removing counts from the 979-keV peak. The summing correction for the 1069-keV peak is more serious: About 35% of the counts in this peak are due to summing. For the γ rays above 2 MeV shown in Fig. 7, the summing effects are small compared to the statistical uncertainties in the yields, because for these lines the major γ-ray branch of the particular ^{25}Na level is to the ground state. A further complication is that the composite relative efficiency curve for geometry 1 obtained from the ^{19}O, ^{24}Na, and ^{25}Na lines, is itself distorted by summing effects. The final uncertainties presented in the intensities of the lines above 2 MeV reflect consideration of these effects.

However, the relative intensities of the 89-, 979-, and 1069-keV lines are important numbers needed in order to evaluate the major β branches of ^{25}Ne, and indeed to deduce a mass for ^{25}Ne by β-γ coincidence work. Measuring the spectrum of β rays in coincidence with the 89-keV γ ray does not directly measure the mass of ^{25}Ne because of the chance that the 89-keV γ ray was part of the 1069-89-keV cascade following β decay to the 1069-keV level in ^{25}Na. For this reason, the relative intensities of the three major lines was remeasured in two other geometries.

IV. RESULTS WITH GEOMETRIES 2 AND 3

Geometry 2 is that shown in Fig. 8, except that the Ge(Li) detector was moved back as additional 4.1 cm from its position indicated in Fig. 8. For both of these geometries the counting cell was 7.6 cm in diameter by 2.5 cm thick. γ rays yields up to 1.8 MeV were remeasured with geometry 2. A composite relative efficiency curve was obtained from the internal ^{19}O, ^{24}Na, and ^{25}Na lines as before, and in addition an absolute efficiency curve was obtained from International Atomic Energy Agency standard γ-ray sources. To simulate the geometry, the intensity calibration sources were held at a position equivalent to the center of the gas counting chamber and moved transversely to effectively cover the entire 7.6-cm diameter of the counting cell. Photofractions were also obtained by computing the ratio of peak counts to total counts in the calibration spectra. With this information, the summing effects could be computed with adequate precision and amounted to a summing loss of 1.2% for the 979-keV line and an 8% correction to the 1069-keV yield.

The Ge(Li) counter was then moved up to the position shown in Fig. 8 and the γ-ray yields were remeasured. Internal relative efficiency and external absolute efficiency curves and photofractions were obtained for this geometry as before. The relative intensities of the 89-, 979-, and

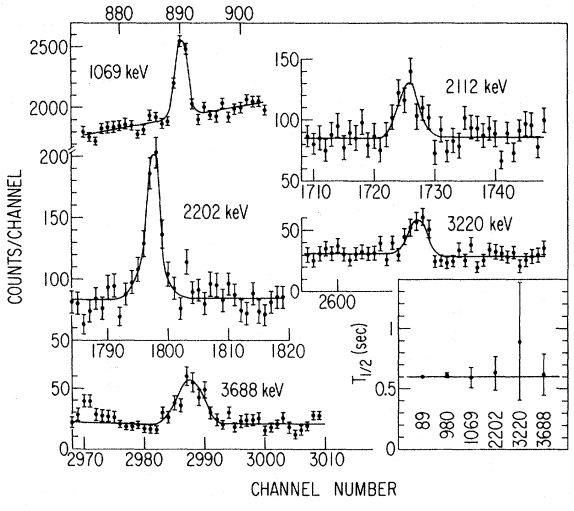

FIG. 7. The spectra of high-energy γ rays from the decay of ^{25}Ne. The solid curves away from the peaks represent the backgrounds used to estimate the γ-ray yields. The numbers below each plotted half-life denote the energy of the corresponding line. The values for the half-lives for the 89-, 980-, and 1069-keV transitions include data from other runs. The half-life deduced for the 2112-keV line is less than 4.3 sec, with 85% confidence.

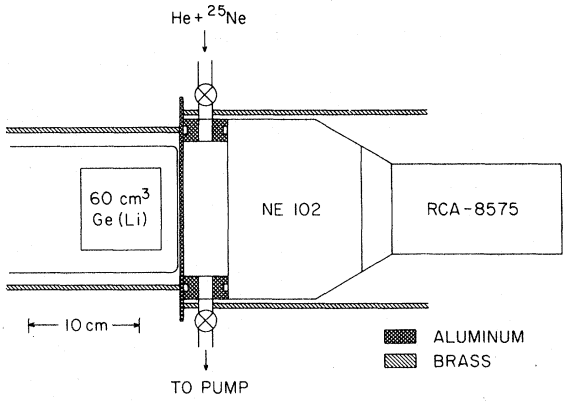

FIG. 8. The counting cell for geometry 3. Geometry 2 is identical except that the Ge(Li) detector was moved an additional 4.1 cm away from the gas cell. The latter was sealed with an O-ring directly onto the aluminized front face of the NE102 scintillator, which was 10.2 cm in diameter and 7.6 cm deep. A short Lucite light pipe joined the scintillator to the photomultiplier tube. Brass shields around the Ge(Li) detector and the NE102 detector prevented Pb x rays from nearby lead bricks from entering the Ge(Li) detector.

1069-keV lines, when corrected for summing, agreed within errors with the values determined in the geometry 2 runs. The summing corrections are calculated on the basis of an isotropic correlation between the 979- and 89-keV γ rays (see Fig. 1). If the spin of the 89-keV level is $\frac{3}{2}^+$, as is most probable, and if both transitions are dipole, then the unperturbed correlation between the two is $1+0.05P_2(\cos\theta)$. If the spin of the 89-keV level is $\frac{5}{2}^+$ and the second transition is dipole, the unperturbed correlation is $1+0.2P_2(\cos\theta)$. In addition, the mean lifetime of the 89-keV level is 7.3 nsec,[9] so that the true correlation is more isotropic than the above values. The uncertainties in the angular correlation make a negligible uncertainty in the summing corrections.

The relative intensities of the 89- and 979-keV γ rays from the above runs indicated a β branch to the 1069-keV level of about one fifth the strength of the β branch to the 89-keV level.

The combined results for the β- and γ-ray intensities for the three geometries are shown in Table I. Values for γ-ray energies are also given in the table. The energy of the 89-keV γ ray was obtained by several different methods. The ^{25}Ne (89-keV) line was counted simultaneously with the ^{203}Hg (72.87- and 279.19-keV)[16] lines and the ^{19}O (109.89- and 197.148-keV)[15] lines. The 89-keV γ ray was recalibrated with the ^{19}O lines in three other runs with different geometries and amplifiers. All results agreed well within the 100-eV uncertainty quoted for this line in Table I. The 979.77 $\pm$0.16-keV line was measured several times using the 974.71$\pm$0.12-keV[14] line from ^{25}Na (see Fig. 5) for calibration.

V. COINCIDENCE MEASUREMENTS OF β-RAY SPECTRA

Using geometry 3 as shown in Fig. 8, β-ray singles, γ-ray singles, and β-ray pulses in coincidence with various digital windows set on γ-ray photopeaks and backgrounds were simultaneously counted. Figures 4 and 5 show the location of digital windows on the 89- and 979-keV peaks and backgrounds, respectively. Each of the three types of events was recorded separately in two successive 0.6-sec bins, using the timing sequence shown in the lower part of Fig. 2. Conventional modular electronics were used to create 700-nsec wide bipolar pulses from the NE102 detector for minimum pileup, and with the typical β counting rate of 2500/sec, the reals to randoms ratio exceeded 1000, even though the coincidence resolving time was set at 120 nsec. The time window was set this wide to assure that the timing efficiency was unity down to a γ-ray energy of 75 keV, and to record the 89-keV pulses over 4 mean

TABLE I. β decay of ^{25}Ne to levels of ^{25}Na.

^{25}Na level E_x (keV)	I_β [a] β rays/100 decays	E_γ (keV)	I_γ [a] γ rays/100 decays	E_β(max) (MeV)	$\log_{10} ft$ [a]
0	$\leq$20 [b]			7.4 $\pm$0.3	$\geq$5.0 [b]
89.53 $\pm$0.10	76.8 $\pm$1.9	89.53 $\pm$0.10	95.5 +0.6	7.3 $\pm$0.3	4.45 $\pm$0.09
		979.77 $\pm$0.16	18.1 +1.9		
1069.32 $\pm$0.19 [c]	19.2 $\pm$2.0	1069.30 $\pm$0.19 [c]	2.34 $\pm$0.38	6.3 $\pm$0.3	4.76 $\pm$0.12
		1132.8 $\pm$1.0 [d]	0.4 $\pm$0.3		
		2112.5 $\pm$1.0 [e]	0.62 $\pm$0.19		
2202.1 $\pm$1.0	2.3 $\pm$0.5	2202.0 $\pm$1.0	1.1 $\pm$0.3	5.2 $\pm$0.3	5.3 $\pm$0.2
2417 $\pm$3 [f]	$\leq$0.40 [b]	2417 $\pm$3	$\leq$0.40 [b]	5.0 $\pm$0.3	$\geq$5.9 [b]
2788 $\pm$3 [f]	$\leq$0.32 [b]	2788 $\pm$3	$\leq$0.32 [b]	4.6 $\pm$0.3	$\geq$5.9 [b]
2914 $\pm$3 [f]	$\leq$0.41 [b]	2825 $\pm$3	$\leq$0.41 [b]	4.5 $\pm$0.3	$\geq$5.7 [b]
3353 $\pm$3 [f]	$\leq$0.51 [b]	3353 $\pm$3	$\leq$0.46 [b]	4.0 $\pm$0.3	$\geq$5.4 [b]
		3599 $\pm$3 [g]	0.22 $\pm$0.16		
3688 $\pm$3	1.18 $\pm$0.30	3688 $\pm$3	0.96 $\pm$0.24	3.7 $\pm$0.3	4.9 $\pm$0.2
(4289 $\pm$3) [h]	($\geq$0.52 $\pm$0.15) [i]	(3220 $\pm$3)	(0.53 $\pm$0.15)	(3.1 $\pm$0.3)	(4.9 $\pm$0.5)

[a] These values assume I_β=0 to the ^{25}Na ground state.
[b] These limits are taken at the 85% confidence level.
[c] Calculated from γ(89) + γ(979).
[d] Calculated from γ(1069) + γ(2202).
[e] Calculated from γ(89) + γ(2202).
[f] Taken from Ref. 9.
[g] Calculated from γ(89) + γ (3688).
[h] Calculated from γ(1069) + γ(3220). This β branch is not definite.
[i] This value is only a limit because the γ-ray branching of the 4289-keV level is not known.

lives of the 89-keV level, ($T_m = 7.3 \pm 0.7$ nsec[9]).

Pulses in the NE102 scintillator were counted in coincidence with the 89-, 979-, and 1069-keV lines from ^{25}Ne, the 440-keV line from ^{23}Ne, the 1612-keV line from ^{25}Na, and the 1357- and 1554-keV lines from ^{19}O. Background spectra for each of the above cases were also stored by using regions just above and below the photopeaks, as illustrated in Figs. 4 and 5. The spectra for the lines from isotopes other than ^{25}Ne were taken to provide calibration β spectra.

The ^{25}Ne β rays were expected to have an end-point energy[7] of about 7 MeV and since the highest energy β end point available in the simultaneous calibration spectra mentioned above was the 3.93-MeV[17] spectrum from ^{23}Ne, it was desirable to obtain a higher-energy calibration point, in particular the 5.393-MeV[17] spectrum from the decay of ^{20}F. After several unsuccessful attempts to produce this activity in the gas counting cell simultaneously with ^{25}Ne by mixed target techniques, a different method was used. The Be target foil was replaced by a Pt foil and the beam changed to 4-MeV deuterons. The helium sweeping gas was replaced by a mixture of 90% neon and 10% SF_6 gas at 1 atm pressure. This permitted the simultaneous counting of ^{20}F and ^{23}Ne activities, produced by the ^{19}F(d, p) and ^{22}Ne(d, p) reactions, respectively. The β spectra were counted in coincidence with digital windows on the corresponding 1633- and 440-keV γ-rays peaks and backgrounds. The purpose of counting the ^{23}Ne activity together with the ^{20}F activity was to allow higher count rates to be used without concern as to count-rate dependent gain shifts, since a ^{23}Ne spectrum was recorded simultaneously with the ^{25}Ne β spectra in the runs carried out earlier. Figure 9 shows the upper portion of the 5393-keV (Ref. 17) ^{20}F β spectrum. The lower part is not shown, as it is distorted by scattering effects. The solid curve is a fit to the data, using an allowed shape function folded into a Gaussian experimental resolution function whose width varied as the square root of the channel number to simulate phototube statistics. The calculated end-point channel is indicated by the arrow, and was insensitive to the fitting region.

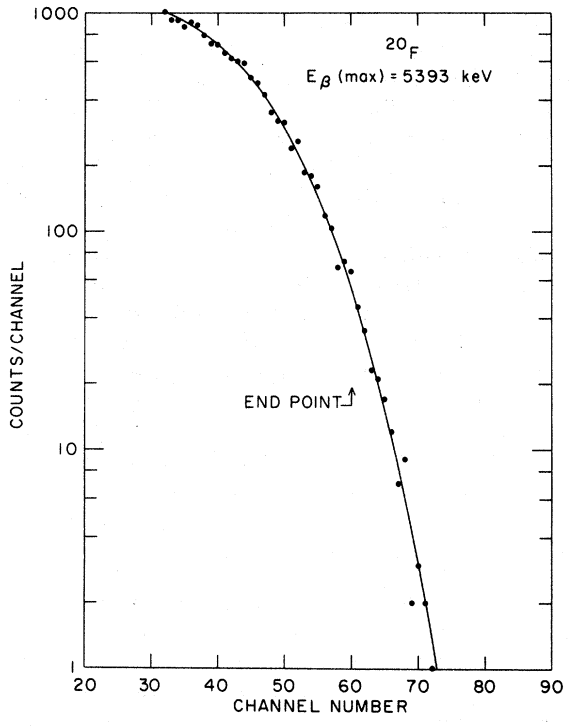

FIG. 9. The ^{20}F calibration β-ray spectrum, taken in geometry 3 with the Ne + SF_6 gas mixture. The counts above channel 62 are due to the experimental resolution.

The spectrum of pulses in the NE102 scintillator in coincidence with 89-keV γ rays contains events due to β rays feeding the 1069-keV level of ^{25}Ne as well as the 89-keV level. In addition, the summing of γ rays and β-ray pulses within the scintillator must also be considered. By numerically integrating over the solid angle of the β counter, one finds that the 89-keV γ ray has about a 17% chance of leaving some energy in the detector, and that the 979-keV γ ray has about a 9% chance. The spectrum of pulses in the NE102 scintillator in coincidence with the 979-keV γ ray was corrected for summing with the 89-keV γ ray. This resulting spectrum of β rays populating the 1069-keV level was then modified by summing into it the response function for a 979-keV γ ray. This result was multiplied by an appropriate factor and subtracted from the spectrum of NE102 pulses coincident with the 89-keV γ ray. Both corrected spectra are shown in Fig. 10. The solid curves are least-squares fits to an allowed shape function folded into the same resolution function that was determined by fitting the ^{20}F β spectrum. Two free parameters, a height normalization and an end-point channel number were used in determining these fits. The arrows indicate the computed end-point channels.

A β-ray calibration curve was then constructed from the computed end points to the data for the 3264-keV end-point[17] spectrum in coincidence with the 1554-keV ^{19}O line, the 3939-keV end-point[17] spectrum coincident with the 440-keV ^{23}Ne line, and the 5393-keV[17] spectrum from ^{20}F. The Compton edge of the 898-keV ^{88}Y line was used to determine the zero intercept. The values determined for the mass of ^{25}Ne from the β_1 and β_2 spectra

agreed within uncertainties, and we deduce a value of Q_β (defined as the end-point β energy to the ground state of ^{25}Na) of 7.4 ± 0.3 MeV. The precision is limited by the statistics on the ^{23}Ne calibration spectrum taken simultaneously with the ^{25}Ne β spectrum, and by the fact that we were unable to simultaneously produce a β spectrum with an end point above 7.4 MeV in the same geometry for calibration.

However, to check for a possible nonlinearity of the scintillator for high-energy β rays, another experiment was carried out. The detector was placed 20 cm from targets of BaF_2 or ^{14}C, which were bombarded with 3-MeV deuterons on the BNL 3.5-MeV Van de Graaff. β rays were viewed through a 0.25-mm Be exit window. The 1.5-mm-thick aluminum plate shown as the gas cell cover in Fig. 8 was replaced by 0.025 mm of aluminum. Delayed β spectra from ^{20}F and ^{15}C (end point 9.77 MeV)[17] were recorded in the scintillator as singles in various time bins. The detector was sufficiently far from the targets that γ-ray summing was negligible. Background spectra due to cosmic rays were measured and used to correct the raw spectra. The computed β end points for these two spectra showed no evidence for nonlinearity within the precision of the results, i.e., about 2.5%, after corrections were made for β-ray energy loss in the Be and Al foils and the intervening air.

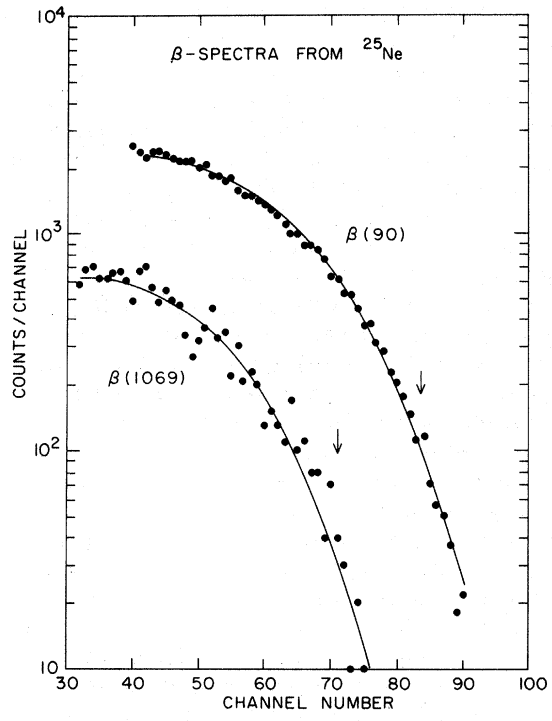

FIG. 10. ^{25}Ne β-ray spectra to the 90- and 1069-keV levels of ^{25}Na. The solid lines are two-parameter fits to the data. For the β(1069) data the scale on the left should be divided by 10. The dispersion is about 90 keV/channel.

VI. LIMIT ON THE GROUND-STATE β BRANCH

Since the half-life of ^{25}Na is 100 times that of ^{25}Ne, and since the former is made directly by the ^{9}Be(^{18}O, pn) reaction, it is exceedingly difficult to provide a reasonable measure of the ground-state β branch by observing the buildup in time of the daughter activity.

A measure of this desired branch is contained in the β-ray singles spectra that were recorded simultaneously with the coincidence work. By considering only pulses in channel numbers >63, most of the events due to ^{19}O, ^{23}Ne, ^{24}Ne, and ^{25}Na could be excluded in the singles spectra. The yield of singles pulses above channel 63 was computed by subtracting the events in the second time bin from those of the first bin. In this way, long-lived activities such as cosmic-ray induced pulses were subtracted out of the singles spectrum. The number of pulses in this resultant spectrum that could be accounted for by the β rays feeding the 1069- and 89-keV levels was calculated, using the measured γ-ray efficiency curve and considering γ-ray summing effects in the NE102 scintillator for both singles and coincident spectra.

The result is that $\beta_0/\beta_1 = 0.17 \pm 0.09$. We do not interpret this result as indicating a ground-state β branch, because of the possibility that the β singles spectra above channel 63 contained an excess of events over that from ^{25}Ne due possibly to small pileup effects or short-lived background. Also, if the lifetime of the 89-keV level were longer than 8 nsec, our coincidence efficiency would be lower than unity, resulting in an apparent ground-state β branch. This result does, however, provide a firm upper limit of 0.26 for the ratio β_0/β_1. Using the values in Table I, this corresponds to a limit of 0.20 for the ratio of β_0 to the sum of all β, with 85% confidence.

VII. DISCUSSION OF RESULTS

Table I and Fig. 11 summarize the results of this work. The spin of ^{25}Ne is established to be $J^\pi = \frac{1}{2}^+$ or $\frac{3}{2}^+$ by the existence of the allowed decay to the 1069-keV level. The parity of the 2202-keV level is assigned as positive and the assignments for the spin of the 3688-keV level are based upon the allowed logft values. A tentative transition to the state at 4289 keV is indicated.

Our result of 7.4 ± 0.3 MeV for Q_β is to be compared with the value of 7.1 ± 0.3 MeV reported by Kabachenko *et al.*[7] for the effective end point of their singles β spectrum. Adding 90 keV to their result, assuming no ground-state β branch, we interpret their data as indicating a value for Q_β of about 7.2 ± 0.3 MeV. One would also expect their result to be lower than ours because of the interference in their singles β spectrum of the branch to the 1069-keV level. Our value for Q_β corresponds to a mass excess for ^{25}Ne of -1.96 ± 0.30 MeV. This value is to be compared with the original prediction of -1.94 MeV by Garvey *et al.*,[8] and -1.28 MeV as recently predicted by Thibault and Klapisch,[18] who used Garvey's formalism with more recently reported mass measurements.

A rough value for the cross section for the ^{9}Be(^{18}O, $2p$)^{25}Ne reaction has been obtained. As noted before, the entire target foil is effective and assuming that the efficiency for collecting the ^{25}Ne recoils into the counting chamber is just the volumetric efficiency, our results indicate an average cross section from 27–44 MeV in the lab (9.0–14.7 MeV in the c.m.) of 26 μb, with an uncertainty of a factor of 2. The Coulomb barrier in the c.m. is about 8 MeV, and the Q value for the reaction is -2.05 ± 0.30 MeV, so that it is reasonable to expect most of the cross section to occur between 9 and 15 MeV in the c.m. An excitation function with the 2.1-mg/cm^2 target showed that the ^{25}Ne yield did maximize at 44 MeV (lab), but that it was not very sensitive to the beam energy.

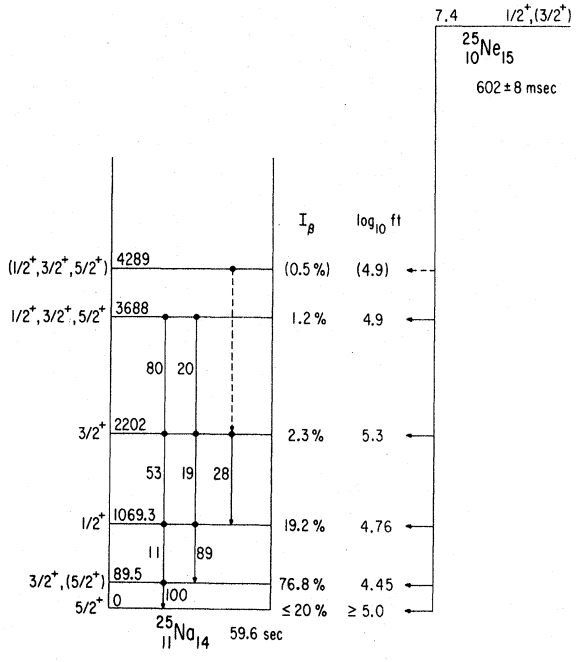

FIG. 11. The decay scheme of ^{25}Ne. The information on ^{25}Na includes the results of the present work and those summarized in Ref. 9.

A. Shell-Model Interpretation

The spherical shell model predicts $J^\pi = \frac{1}{2}^+$ for ^{25}Ne(0), consisting of a $d_{5/2}{}^2$ proton and $d_{5/2}{}^6 s_{1/2}{}^1$ neutron configuration. Elliot and Lane[19] have pointed out that jj coupling is a better approximation for higher isobaric spin, and since ^{25}Ne has $T = \frac{5}{2}$, one would in this spirit expect the above configuration to be the major component of the ^{25}Ne(0) wave function. Experimentally, the ^{27}Mg(0) spin is $\frac{1}{2}^+$, and its configuration is this model is simply the addition of two more protons to the $d_{5/2}$ shell. In fact, the β decay of ^{27}Mg is quite similar to that observed for ^{25}Ne.

The shell-model prediction for the ^{25}Na ground state is a $d_{5/2}{}^3$ proton and $d_{5/2}{}^6$ neutron configruation. Becker *et al.*[9] have pointed out the striking similarity between the low-lying levels of ^{25}Na and ^{19}O, the latter of which is obtained simply by removing the entire closed $d_{5/2}{}^6$ neutron shell from ^{25}Na and invoking charge independence to predict that the levels of the $d_{5/2}{}^3$ configuration are the same for ^{19}O as for ^{19}Na. Properly antisymmetrized states of the $d_{5/2}{}^3$ configuration (with $T = \frac{3}{2}$) can exist only for states with spin and parity $\frac{3}{2}^+$, $\frac{5}{2}^+$, and $\frac{9}{2}^+$. As was pointed out by Becker *et al.*,[9] it is natural to assign the $J = \frac{3}{2}$ member of this configuration to the 96-keV ^{19}O ($\frac{3}{2}^+$) level and to the 90-keV ^{25}Na level. However, the predicted β branch between the ^{25}Ne(0) and ^{25}Na(90) levels in this model is zero, yet a transition with logft = 4.4 is observed. It is apparent that other components are needed in the wave functions for either or both of the above levels.

If the $\frac{1}{2}^+$ level in ^{25}Na is assigned the $d_{5/2}{}^2 s_{1/2}$ proton and $d_{5/2}{}^6$ neutron configuration, then the branch coupling ^{25}Ne(0) to ^{25}Na(1069) has a predicted logft of 3.1. This is a much stronger branch than that observed, but if both wave functions have amplitudes of 0.4 for being pure $s_{1/2}$ states, then the predicted logft would equal that observed, namely 4.7.

It is very apparent that detailed mixing calculations are needed in order to describe the experimental situation in the shell-model basis.

B. Strong Coupling Model Interpretation

A discussion of the low-lying levels of ^{25}Mg and ^{25}Na(0) in terms of the strong coupling rotational model has been given by Litherland *et al.*,[20] and more recently by Morrison *et al.*,[21] and Jones *et al.*[22] In order to explain the β decay of the ^{25}Na

ground state to reasonably well-established rotational bands in ^{25}Mg with $K=\frac{1}{2}$ and $\frac{5}{2}$, one needs a $K=\frac{3}{2}$ component in the ^{25}Na(0) wave function. Also, the spin of ^{25}Na(0) is $\frac{5}{2}^+$, so that band mixing is needed to explain the order of levels in ^{25}Na. Morrison *et al.*[21] consider the major component of the ^{25}Na(0) wave function to be the $J=\frac{5}{2}$ rotational member of a mixed $K=\frac{3}{2}, \frac{5}{2}$ band, with the ^{25}Na(89) level being the $J=\frac{3}{2}$ member of the $K=\frac{3}{2}$ band. The reason for the $K=\frac{3}{2}$ band head being situated above its $J=\frac{5}{2}$ member is explained in Refs. 20 and 21 as an assumed Coriolis band mixing due to the close proximity between the unperturbed positions of the $J=\frac{5}{2}$, $K=\frac{3}{2}$ level with the $K=\frac{5}{2}$ band head. Figure 12 shows the suggested major components of the wave functions for the relevant ^{25}Ne and ^{25}Na levels in terms of the Nilsson orbits.[23] The number for each orbit is that given by Nilsson[23] and values of $\Omega=K$ (axial symmetry is assumed) are given to the right of each orbit. The ordering of the orbits is determined by the deformation η which can be limited by the following consideration. ^{25}Ne(0) decays to the $J^\pi=\frac{1}{2}^+$ level in ^{25}Na at 1069 keV, so that the spin of ^{25}Ne(0) is not $\frac{5}{2}^+$. From Fig. 12 this means that $\eta \leq 3$. A spin of $\frac{1}{2}^+$ for ^{25}Ne(0) would be predicted in this simple model for $-5 \leq \eta \leq 3$. A spin of $\frac{3}{2}^+$ is predicted if $\eta < -5$.

Using the wave functions of Nilsson[23] we have calculated the predicted logft values for β decay of the ground state of ^{25}Ne to the 89-, 1069-, and 2202-keV levels in ^{25}Na using the configurations in Fig. 12. The 2202-keV level has $J^\pi=\frac{3}{2}^+$ and is assumed to be the second member of the $K=\frac{1}{2}$ band starting at 1069 keV. Calculations were also performed assuming that ^{25}Ne(0) has $J=\frac{3}{2}$ based upon Nilsson orbit 8 with $\eta=-6$. Logft values were computed for final state deformations ranging from $-6 \leq \eta \leq 6$. These calculations assumed that the remaining 24 nucleons stayed in their original orbits. The only region where respectable agreement with the three experimental values was obtained was near η (^{25}Ne) = 1 and η (^{25}Na) = 6. The latter deformation is also that value used by Ref. 21 in calculating the β decay of ^{25}Na and ^{25}Si. However, in this simple model, the remaining 24 nucleons would not remain in their original orbits, since for $\eta=6$ orbit 9 is situated below orbit 5. Thus one would expect that for ^{25}Na with $\eta=6$ there would be two neutrons in orbit 9 and none in orbit 5. Since the Gamow-Teller operator is only a one-body operator, transitions between ^{25}Ne with $\eta<3$ and ^{25}Na with $\eta>3$ would then be forbidden, since it requires changing the orbits of 3 nucleons.

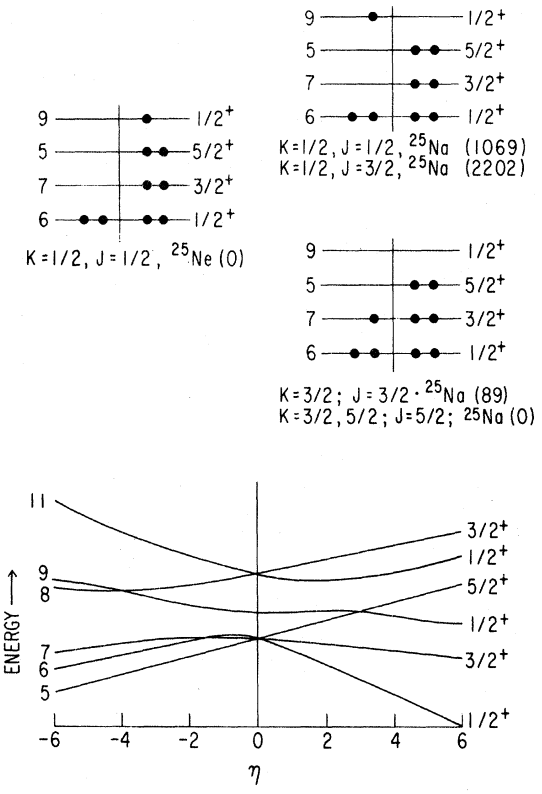

FIG. 12. Nilsson configurations for the major components of ^{25}Ne and ^{25}Na levels, as suggested by the results of this work and previous information. Orbits 1–4 are filled. $J^\pi=\frac{1}{2}^+$ states in ^{25}Na can also be constructued by exciting a proton from orbit 6 into orbit 7, but this configuration could not be populated by allowed decay from the hypothesized ^{25}Ne(0) configuration. The lower plot of energy vs deformation is taken from Ref. 23. The ordering of orbits 9 and 5 depends upon the deformation, and the configurations are shown for $0<\eta<3$.

For $\eta<3$, there is no region within our calculations where respectable agreement with the three measured values results. The simple Nilsson model used neglects Coriolis band mixing as well as the J^2 term in the particle Hamiltonian.[24] Hopefully more sophisticated calculations can further explain this situation.

ACKNOWLEDGMENTS

We are thankful to Dr. D. Kurath for discussions concerning the limitations of the simple Nilsson model to the mass-25 region, and to Dr. J. D. Larson, for his assistance in least-squares fitting of the β-ray spectra including resolution with DESCALC.

*Work performed under the auspices of the U. S. Atomic Energy Commission.

[1]D. R. Goosman and D. E. Alburger, Phys. Rev. C 6, 825 (1972).
[2]D. R. Goosman and D. E. Alburger, Phys. Rev. C 5, 1252 (1972).
[3]D. R. Goosman and D. E. Alburger, Phys. Rev. C 6, 820 (1972)
[4]A. G. Artukh, V. V. Avdeichikov, G. F. Gridnev, V. L. Mikheev, V. V. Volkov, and J. Wilczynski, Phys. Letters 31B, 129 (1970).
[5]A. G. Artukh, V. V. Avdeichikov, G. F. Gridnev, V. L. Mikheev, V. V. Volkov, and J. Wilczynski, Nucl. Phys. A176, 284 (1971).
[6]R. Klapisch, C. Thibault-Philippe, C. Detraz, J. Chaumont, and R. Bernas, Phys. Rev. Letters 23, 652 (1969).
[7]A. P. Kabachenko, I. B. Kyznetzov, K. Sivek-Vilchinka, E. A. Skakun, and N. I. Tarantin, Joint Institute for Nuclear Science, Dubna Report No. D7-5769, 1971 (unpublished), p. 204.
[8]G. T. Garvey, W. J. Gerace, R. L. Jaffe, I. Talmi, and I. Kelson, Rev. Mod. Phys. Suppl. 41, S1 (1969).
[9]J. A. Becker, R. E. McDonald, L. F. Chase, Jr., and D. Kohler, Phys. Rev. 188, 1783 (1969); and J. A. Becker, private communication.
[10]S. Hinds, H. Marchant, and R. Middleton, Nucl. Phys. 31, 118 (1962).
[11]J. E. Esterl, R. G. Sextro, J. C. Hardy, G. J. Ehrhardt, and J. Cerny, Nucl. Instr. Methods 97, 229 (1971).
[12]L. C. Northcliffe and R. F. Schilling, Nucl. Data A7, 233 (1970).
[13]G. E. Schwender, D. R. Goosman, and K. W. Jones, Rev. Sci. Instr. 43, 832 (1972).
[14]D. E. Alburger and D. H. Wilkinson, Phys. Rev. C 3, 1957 (1971); see also Ref. 22.
[15]F. Ajzenberg-Selove, Nucl. Phys. A190, 1 (1972).
[16]J. B. Marion, Nucl. Data A4, 301 (1968).
[17]A. H. Wapstra and N. B. Gove, Nucl. Data A9, 277 (1971).
[18]C. Thibault and R. Klapisch, Phys. Rev. C 6, 1509 (1972).
[19]J. P. Elliot and A. M. Lane, in *Handbuch der Physik*, edited by S. Flugge (Springer-Verlag, Berlin, Germany, 1957), Vol. 39, p. 350.
[20]A. E. Litherland, H. McManus, E. B. Paul, D. A. Bromley, and H. E. Gove, Can. J. Phys. 36, 378 (1958).
[21]G. C. Morrison, D. H. Youngblood, R. C. Bearse, and R. E. Segel, Phys. Rev. 174, 1366 (1968).
[22]A. D. W. Jones, J. A. Becker, R. E. McDonald, and A. R. Poletti, Phys. Rev. C 1, 1000 (1970).
[23]S. G. Nilsson, Kgl. Danske Videnskab. Selskab, Mat.-Fys. Medd. 29, No. 16 (1955).
[24]J. P. Davidson, *Collective Models of the Nucleus* (Academic, New York, 1968), p. 67.

PHYSICAL REVIEW C VOLUME 7, NUMBER 3 MARCH 1973

Mass-25 Isobaric Multiplets*

W. Benenson, E. Kashy, and I. D. Proctor
Cyclotron Laboratory, Michigan State University, East Lansing, Michigan 48823
(Received 19 October 1972)

High-precision mass determinations have now been made for all four members of the lowest two $T = \frac{3}{2}$ states in the $A = 25$ system. The results are used to compute the coefficients of the isobaric-mass-multiplet equation.

I. INTRODUCTION

The isobaric-mass-multiplet equation relates the masses of the $2T+1$ members of a multiplet with isobaric spin T. The equation is usually given as

$$M(T_z) = a + bT_z + cT_z^2,$$

where T_z is the z component of the isobaric spin, $T_z = \frac{1}{2}(N - Z)$. The coefficients a, b, and c are functions of the mass number A and spin J^π of the levels as well. The equation, in principle, relates the masses of any multiplet of analogous levels.

Deviations from the predictions of the isobaric-multiplet equation are usually measured by citing the magnitude of d, the coefficient of a cubic term required to fit the masses. In terms of the measured masses $M(T_z)$, the d coefficient has a very simple form for a $T = \frac{3}{2}$ system, i.e.,

$$d = \tfrac{1}{6}\{M(\tfrac{3}{2}) - M(-\tfrac{3}{2}) - 3[M(+\tfrac{1}{2}) - M(-\tfrac{1}{2})]\},$$

where $M(T_z)$ is the mass of the level in the T_z nucleus.

Thus the result $d = 0$ implies that the spacing between inner members is $\frac{1}{3}$ the spacing between the outer members. One can also see from the above equation that the uncertainty in d is 3 times more sensitive to the accuracy of the masses of the $T_z = \pm\frac{1}{2}$, $T = \frac{3}{2}$ levels than it is to the $T_z = \pm\frac{3}{2}$ levels.

In the present paper we are discussing the lowest two $T = \frac{3}{2}$ levels in the $A = 25$ nuclei. These are the ground and first excited states of ^{25}Si and ^{25}Na and the lowest two $T = \frac{3}{2}$ states in ^{25}Al and ^{25}Mg with